Medium Resolution Spectrometer And AMPIR Installation For The NUCLOTRON

A.B. Kurepin (INR, Moscow)

Round table discussion

JINR, Dubna, 8.07.2005

Investigation of polarization phenomena and nuclear reactions with the Medium Resolution Spectrometer (MRS)

MRS collaboration

G.S. Averichev, A.A. Baldin, S.N. Basylev, V.V. Glagolev, L.B. Golovanov, A.D. Kirillov, M.S. Khvastunov, P.P. Korovin, L.V. Malinina, P.K. Manyakov, E.A. Matyushevsky, Yu.A. Panebratsev, E.B. Plekhanov, V.N. Pechenov, N.M. Piskunov, P.A. Rukoyatkin, A.V. Shabunov, S.S. Shimanskiy I.M. Sitnik, E.A. Strokovsky, M.V. Tokarev, Yu.A. Troyan, V.I.Yurevich

Laboratory of High Energies, JINR, Dubna, Russia

V.Yu. Alexakhin, N. Angelov, L.S. Azhgirey, N.S. Borisov, V.M. Grebenyuk, V.P. Nomokonov, E.A. Pasyuk, G.D. Stoletov, Yu.A. Usov

Laboratory of Nuclear Problem, JINR, Dubna, Russia

M.G. Sapozhnikov

Laboratory of Particle Physics, JINR, Dubna, Russia

I.V. Puzynin, E.A. Ayrjian, A.V. Fedorov, A.P. Sapozhnikov

Laboratory of Computing Techniques and Automation, JINR, Dubna, Russia

F.F. Guber, A.N. Aseev, Yu.K. Gavrilov, M.B. Golubeva, S.N. Filippov, T.L. Karavicheva, A.b. Kurepin, M.A. Prohvatilov, V.I. Razin, A.I.Reshetin, K.A. Shileev, V.V. Tiflov, N.S. Topilskaja, N.S. Zaikovskaja

Institute for Nuclear Research, Moscow, Russia

A.A. Lukhanin, M.P. Rekalo

National Science Center-Kharkov Institute of Physics and Technology, Kharkov, Ukraine

C.L. Morris, R.L. Boudrie

Los Alamos National Laboratory, Los Alamos, USA

C.F. Perdrisat

College William & Mary, Williamsburg, USA

V. Punjabi

Norfolk State University, Norfolk, USA

R.J. Peterson

Colorado University, Colorado, USA

S. Nedev

High Institute of Chemical Technology, Sofia, Bulgaria

L. Penchev

Institute for Nuclear Research and Nuclear Energy, Sofia, Bulgaria

G. Martinska

University of P.J.Safarik, Kosice, Slovak Republic

PROPOSED EXPERIMENTS

- Deuteron structure in backward elasic scattering

$$\vec{d}+\vec{p} \rightarrow p+d$$

$$\vec{d}+p \rightarrow p+\vec{d}$$

- Strange content of the nucleon

$$\vec{d}+\vec{p} \rightarrow {}^3He+\varphi$$

- Single-spin asymmetries in cumulative particle production

$$d+p \rightarrow h+X \qquad h=\pi^{\pm}, K^{\pm}, p^{\pm}$$

- Strange particle and antibaryon production in relativistic nuclei collisions

$$A+A \rightarrow K^{\pm}(\bar{p}) +X$$

- Excitation of nucleon resonances

$$p\,(d,d'), \qquad A\,(d,d')$$
$$p\,(\alpha,\alpha'), \qquad A\,(\alpha,\alpha')$$

- Excitation of exotic narrow resonances

Medium-Resolution Spectrometer

1..Overall dimensions:	9.25x4.0x5.5 m (length,width,height)
2.Optical configuration:	$QD\overline{D}$
3.Momentum range:	0.2-1.8 Gev/c
4. Nominal momentum (B=17 kGauss):	1500 MeV/c (800 Mev protons)
5. Momentum acceptance:	+- 20% dp/p
6. Momentum resolution:	0.08-0.2 %
7. Solid angle:	7-9 msr
8. Horizontal acceptance angles:	+- 60 mrad
9. Vertical acceptance angles:	+- 40 mrad
10. Total weight:	118 tons
11. Electrial power consumption:	350 kW
12. Voltage: QM01 -123V(100kW), BM01 -204V(161kW), BM02 -127V(89kW)	
13. Water flow:	460 l/min

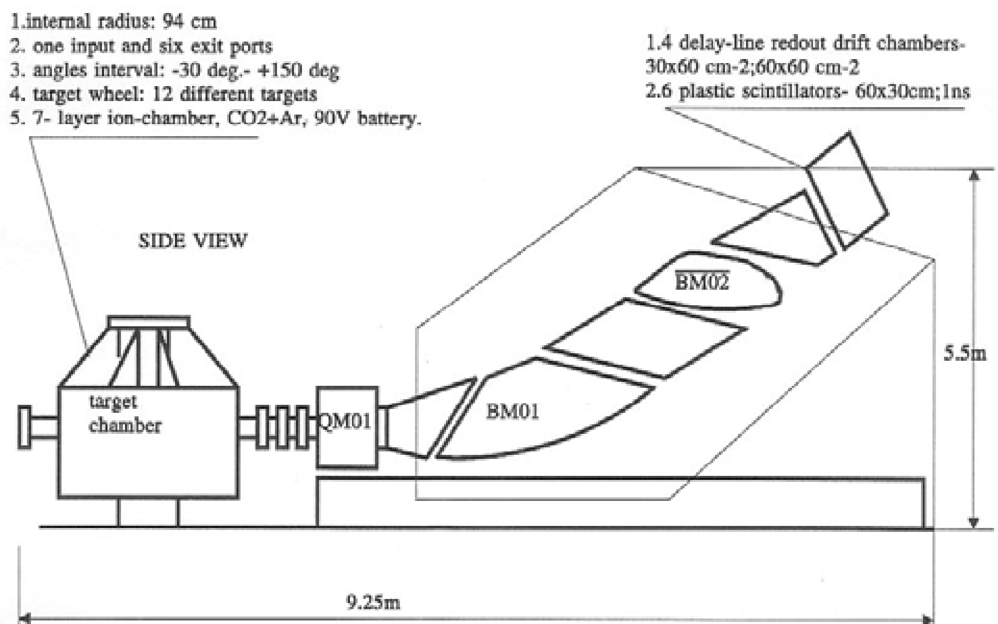

Electronics:

1. Digital micro-VAX IV computer, two 6250 bpi tape drives
2. Three CAMAC crates data acquisition system - A1 controllers
3.Modules:

3 A-1 CC	- crate controller		
1 CES-2180	- Auxiliary CC	1 KS-3610	- input register
1 ECLmean	- 8 channel ECL meantimer	3 Phi 7106	- 16 channel discriminator
1 LRS 4508	- logic unit	1 LRS 2372	- memory lookup unit
1 LRS 4418	- delay unit	4 LRS 4300B	- FERA ADC
3 LRS 4303	- TAC	1 LRS 4301	- FERA driver module
1 LRS 4302	- memory unit	1 LRS 2372	- 32 channel scaler
1 LRS 2551	- 12 channel scaler		

Figure 6: Side view the MRS spectrometer.

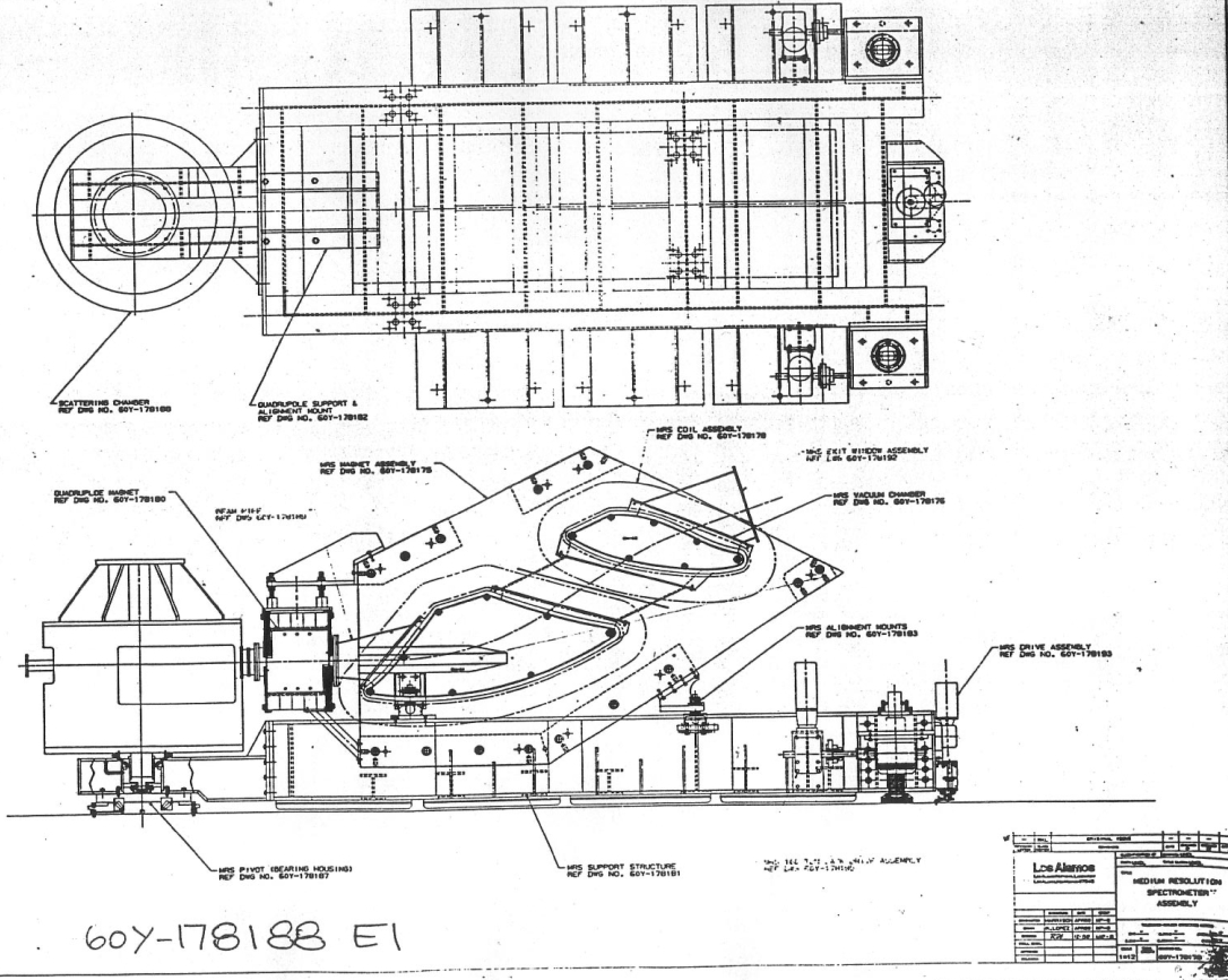

60Y-178188 E1

Table 5: **Main parameters of the MRS**

1.	Overall dimensions (length, width, height), m	 9.25 * 4.0 * 5.5
2.	Optical configuration	$QD\vec{D}$
3.	Momentum range, GeV/c	0.2–1.8
4.	Nominal momentum (B=17 kG), GeV/c	 1.5
5.	Momentum acceptance, $\Delta p/p$, %	±20
6.	Momentum resolution, $\delta p/p$. %	0.08 – 0.2
7.	Solid angle, msr	7 – 9
8.	Horizontal acceptance angles, mr	±60
9.	Vertical acceptance angles, mr	±40
10.	Total weight, tons	118
11.	Electrical power consumption, kW	350
12.	Voltage, V (consumption, kW) Q D $\vec{D}$	 123 (100) 204 (161) 127 (89)
13.	Water flow, l/min	460

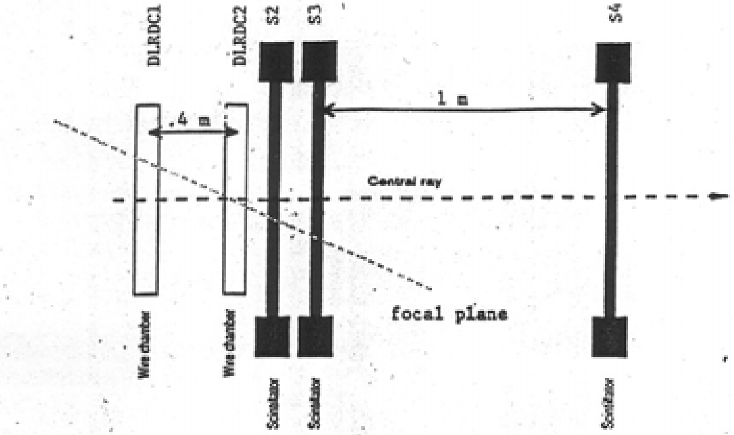

Figure 6: Schematic side view of the MRS spectrometer focal-plane detector system in the standard setup; DLRDC1 and DLRDC2 are delay-line readout drift chamber and S_2,S_3,and S_4 are plastic slab scintillators.

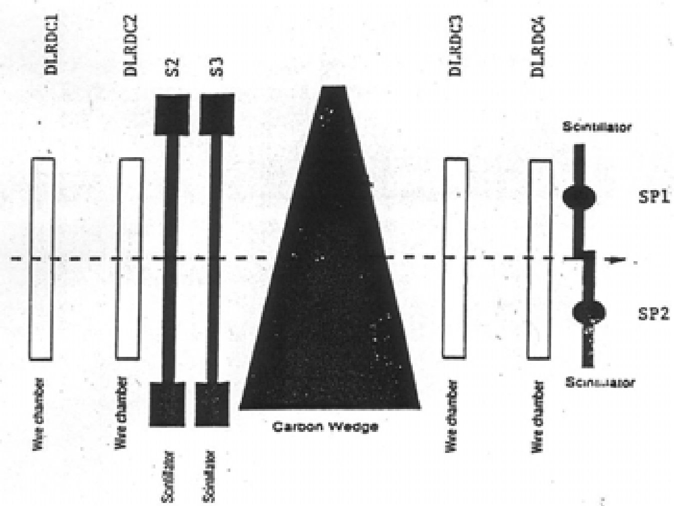

Figure 7: Schematic side view of the MRS spectrometer focal-plane detector system in the focal-plane polarimeter setup; DLRDC1 through DLRDC4 are delay-line readout drift chamber and S_2,S_3,SP_1, and SP_2 are plastic slab scintillators.

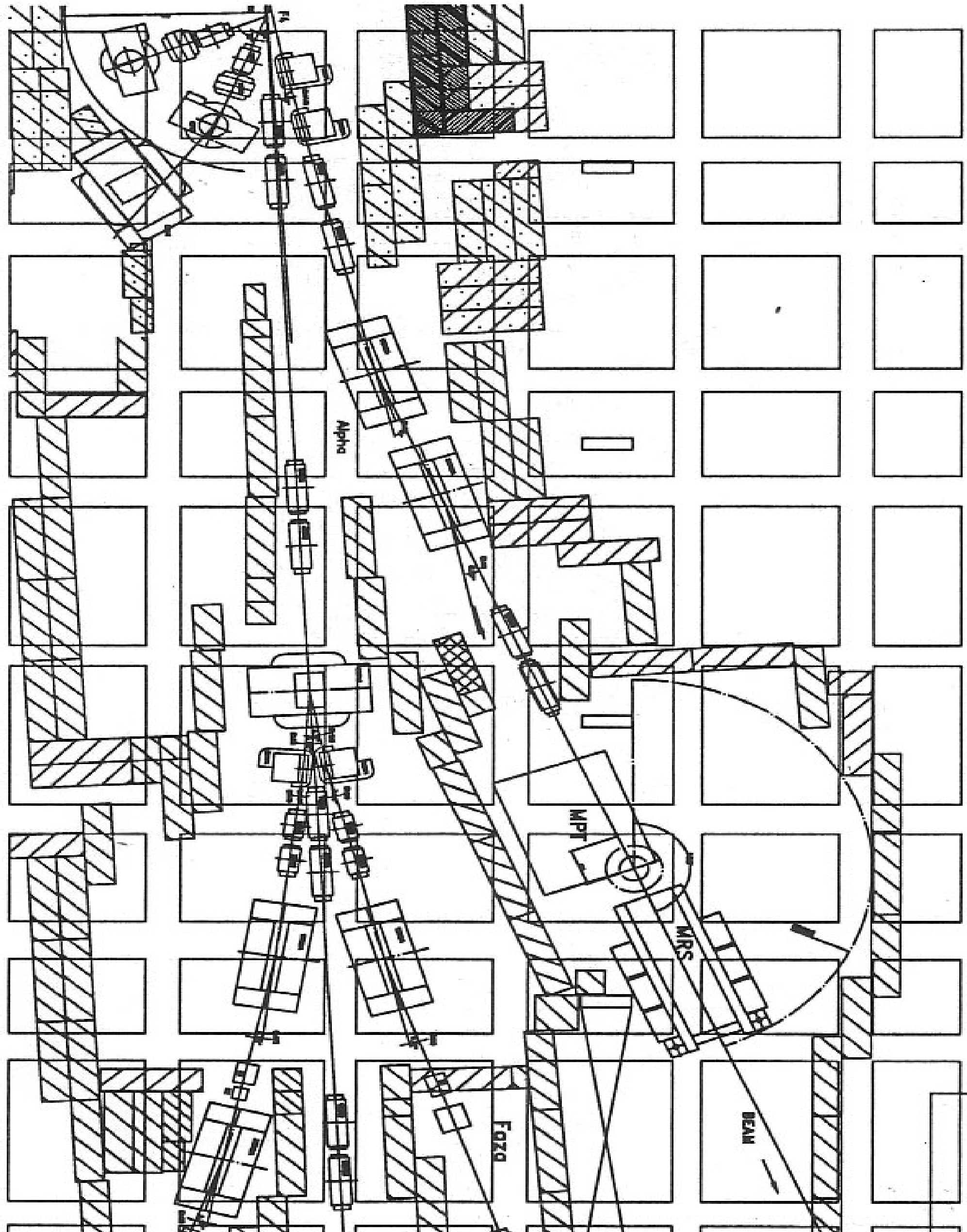

Figure 2: The location of the MRS in the experimental area.

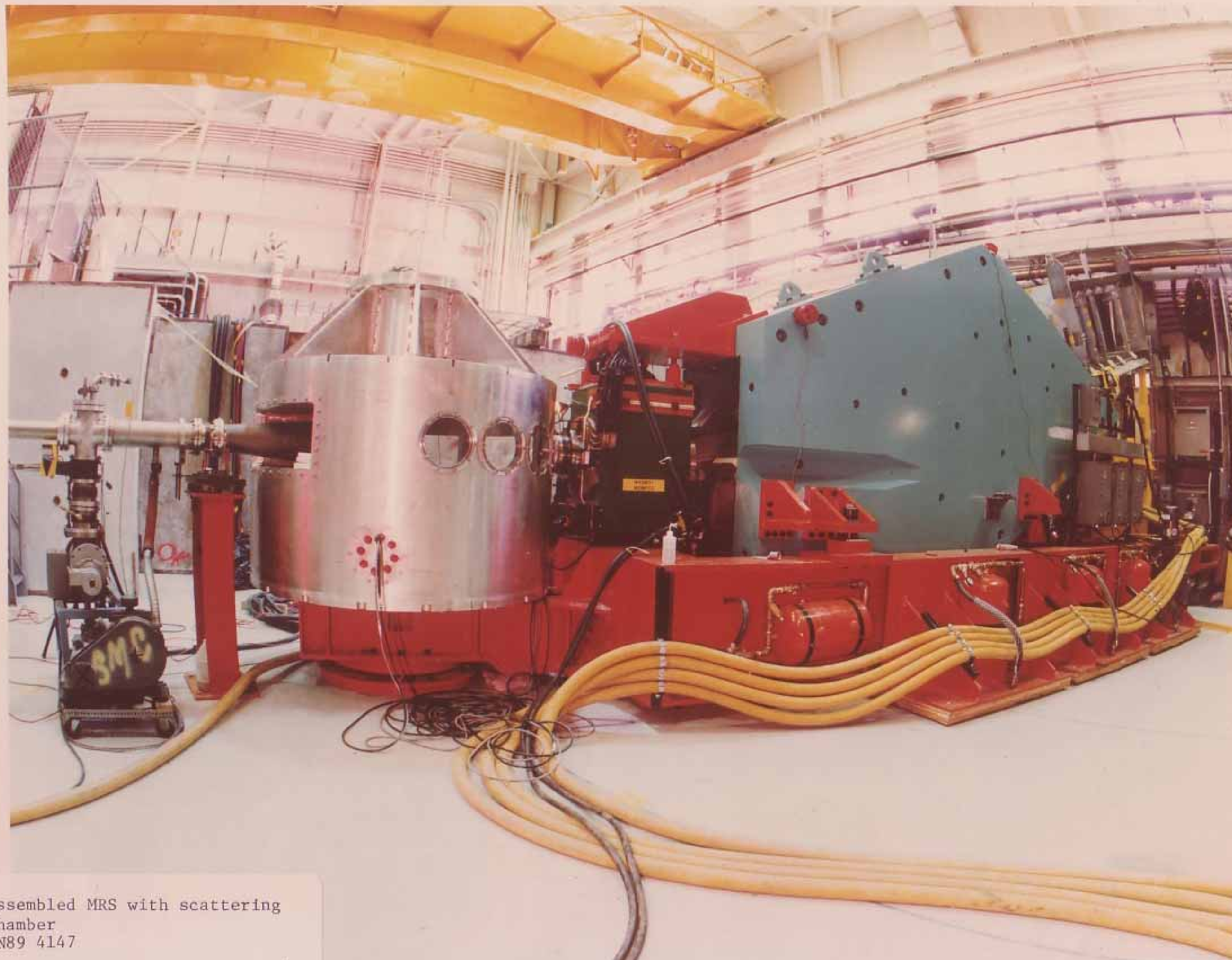

Assembled MRS with scattering
chamber
CN89 4147

8/89

3. Capability to record simultaneously 2 to 8 charged particles with an energy $E \geqslant 20$ MeV and up to 6 γ-rays (2–3– mesons) with energies $E\gamma \geqslant 3$ MeV and $E_{\pi^0} > 0$;

4. Large solid angle of particle detection ($3\pi < \Omega < 4\pi$);

5. Capability to work with various solid and cryogenic targets;

6. High accuracy in determining the vertex of interaction inside the target;

7. Fast electronics slowing the operation with the highintensity ($\cong 10^8$ s^{-1}) beams of primary particles, i.e. the recording of rare events with $\sigma = 1-10$ nbarn.

The individual components of the spectrometer and their current status are described below.

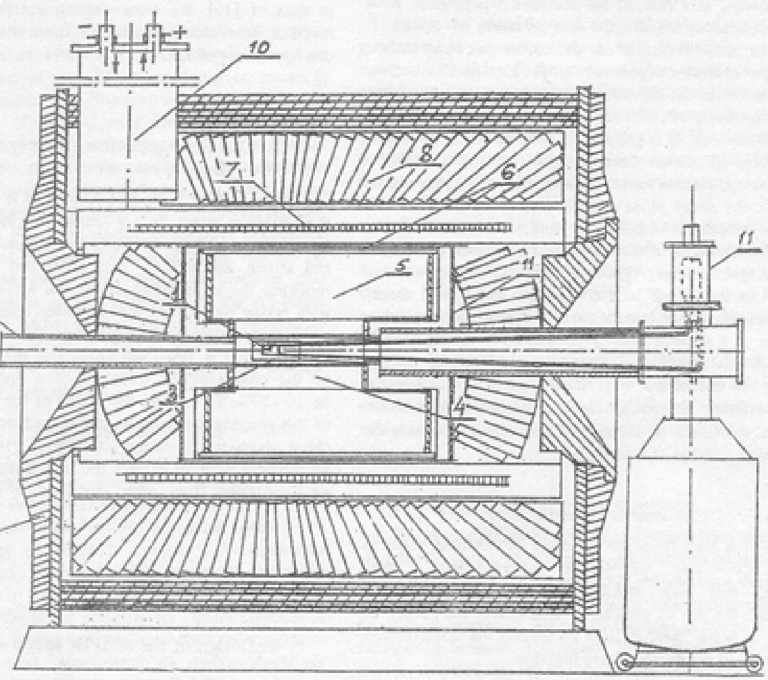

Fig. 1. The lay–out of the AMPOR spectrometer: 1 – target; 2 – vacuum tube; 3 – vertex detector; 4 – internal drift chamber; 5 – 100-cm–long drift chamber; 6 – scintillators; 7 – coil of superconducting solenoid; 8 – neutral particle detector; 9 – magnetic yoke; 10 – cryostat.

2.2. Superconducting magnet

The superconducting radiation–transparent solenoid with an iron magnetic yoke produces at a current of 2.8 kA a magnetic field of 10 kG with a nonuniformity of about 2% in the working volume 0.9 m in deameter and 1 m long.

The solenoid is composed of a selt–supported two–layer edgewise coil made of a superconducting 7x4 – mm² bar (a twist from 8 metal–matrix–composite niobium–titanium wires CKHT–0.7–210–0.5 soldered in a rectangular slot in the middle part of a bimetallic aluminium–copper bar). The bar is insulated by 0.2–mm–thick cotton cloth.

The length of the solenoid is 1800 mm (410 turns per layer), its inner diameter is 1144 mm. The energy stored in a magnetic field of 10 kG. is about 0.74 MJ.

The method of indirect cryostating is used to cool the solenoid. Liquid helium is fed through inlet headers, flows inside 24 parallel thin–walled aluminium 12–mm–diameter pipes fixed with an epoxy adhesive on the outer and inner surfaces of the coil and is collected in outlet headers.

The thermal insulation of the solenoid consists of socalled mylar blanket made up to several tens of super-insulation layers (10–μm–tick mylar metallized with aluminium on a special biberglass base), a soft nitrogen screen shipped with aluminium pipes with liquid nitrogen, and the second mylar–blanket superinsulation. The outer and inner shells of the cryostat are made of aluminium alloys (Fig. 2).

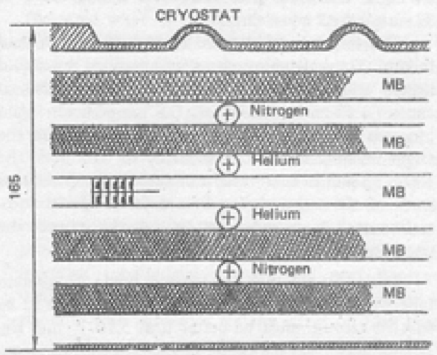

Fig. 2. The schematic of the superconducting solenoid cryostat

To compensate axial and radial forces arising in the magnetic field between the solenoid and the magnetic core poles the solenoid is suspended inside a cryostat by means of fiberglass composite laminate tension members and supports. The cryostat itself is attached to the frame plates of the magnetic core.

The developed designs of the solenoid and the cryostat have a very low absorptivity for γ-rays (0.4 of radiation length).

The 30-t magnetic yoke built up from 11 longitudinal plates and 2 end disks made of CT–10 steel is placed on an alignment base ensuring the positioning and correction of the magnet. The overall dimensions of the magnet are 3350 mm long, 2750 mm high and 2500 mm wide.

The special input unit with electric current leads and a 20–30 l liquid helium tank insulated from external heat by a superinsulation and a nitrogen screen is provided to supply electric power and liquid coolants to the spectrometer. The tank encloses a coil pipe into which liquid helium is pumped to cool the solenoid, and the superconducting sections of the lead conductors. The ends of the conductors soldered to the current leads are cooled with helium from the outlet heads. The helium temperature is 4.6°K at the inlet of the magnet coil 4.7°K at its outlet and no higher that 5.0°K in the "warmest" part. During the primary cooling the intake of liquid helium is provided by bypassing the input unit.

The expected distribution of the magnetic field along the solenoid axis and radius were confirmed by the calculations on the POISSON program for the described design and the simulation experiments at a 1:3 scale "warm" model magnet. It follows from these calculations and measurements that the magnetic field nonuniformity can attain 4–5% at the solenoid ends, but not exceed 2% in the working volume of the detector (l=1 m, d=0.9 m).

The functional test of the solenoid was made with a 1:3 scale superconducting magnet having a coil shown in Fig. 3.

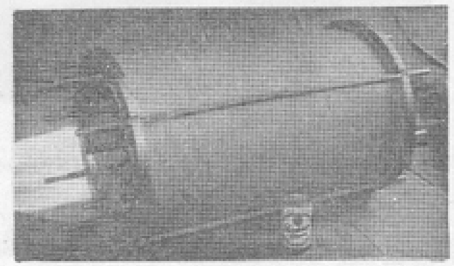

Fig. 3. The coil of the model superconducting solenoid.

2.3. Vacuum tube, target and vertex detector

The vacuum tube enclosing the target and the vertex strip detector in mounted along the solenoid axis and represents a separate leak–tight structure consisting of several sections made of non–magnetic materials. The entrance part equipped with a gate is connected to a ion guide of a pion, proton or photon channel of an accelerator; the central 80-mm-dia part of the vacuum tube (transparent to the reaction products) is made of 700 – m-thick carbon fiber reinforced plastic and connected with the entrance and exit parts by two belows. The exit part of the ion guide is designed to attach the vertex detector, to accommodate its preamplifiers together with cooling pipes and to connect a holder of a cryogenic or solid targets and a beam monitor.

The vertex detector holder represents a light tubular structure on which six paired 60x30–mm² silicon plates 300 m in thickness with longitudinal strips may be mounted (Fig. 4). The slices are attached to glass–cloth–base–laminate frames placed along the beam axis on the generatrices of a 60-mm-dia cylinder. Each slice represents an n-type silicon single crystal with 72 longitudinal p^+–strips 450 m in width ion-implanted in the single crystal surface with a spacing of 500 m. The signal appearing on the strip when a charged particle passes through the slice is supplied to the input of a semiconductor charge-sensitive preamplifier prepared by the hydrid technology. The coordinate of a particle is determined by the triggered channel number and its passage time is established from the pulse arrival moment.